JOURNAL OF MATERIALS SCIENCE 26 (1991) 6547–6552

Organic photovoltaic solar cells based on some pure and sensitized dyes

G. D. SHARMA
Department of Physics, University of Jodhpur, Jodhpur, India
S. C. MATHUR, D. C. DUBE
Department of Physics, Indian Institute of Technology, Delhi-110016, India

Organic photovoltaic solar cells based on metal–dye or sensitized dye–SnO_2 junctions are formed. The electrical and photovoltaic characteristics of these Schottky junctions have been studied on two pure and sensitized dyes (Eriochrome Blue Black B and Rodamine B). From the photovoltaic action spectra the active region responsible for electric power generation was found to be confined to the SnO_2–dye interface. The effect of sensitization, electrode material and intensity on photovoltaic and electrical parameters has also been discussed in detail. Finally the *C–V* characteristics are discussed in detail.

1. Introduction

Thin film organic semiconductors have been extensively used in photography [1], electrophotography [2, 3] and more recently in optical storage systems [4]. In the past few years, there have been several reports on photovoltaic systems involving solid state organic dyes [5–11]. Recent studies [7, 8] revealed that the low efficiency of organic dye solar cells is due to the high resistivity of dye and very high trap density in the forbidden gap which lowers the carrier lifetime. Doping and sensitization in the organic dye resulted in an increase in conductivity. Several workers concluded that in phthalocyanine, there is a drastic improvement in conductivity and photovoltaic behaviour on doping the dye with oxygen and iodine or by sensitization [12, 13].

In the present paper, the results on dark and photoconductivity and photovoltaic studies are reported on pure and sensitized Eroichrome Blue Black B (EBBB) and Rhodamine (RB) dye. The sensitizers used are AgI, AgBr and CdS. The effect of various electrode materials, sensitizers and intensity on the electrical and photovoltaic properties has also been investigated. Various electrical and photovoltaic parameters have been calculated and discussed. Finally the increase in conductivity and photovoltaic performance on sensitization has been discussed with the help of *C–V* characteristics.

2. Experiment

Commercially available organic dyes were first purified by chemical recrystallization followed by chromatography and vacuum sublimation. The thin films of pure and sensitized dyes were prepared by pouring the solution of pure and sensitized dyes, using dimethyl formamide (DMF) as a solvent, onto conducting glass (SnO_2). A finely ground mixture of the dye and the sensitizer in the proportion 3:2 by weight was used for preparation of thin films of the sensitized dye. These films were kept for 24 h for slow evaporation in the solvent atmosphere. When the evaporation was complete, these films were dried at 50 °C for 24 h to remove the traces of solvent in the films. On the other side of these films metal (silver, aluminium and copper) electrodes were vacuum deposited maintaining the vacuum to better than 10^{-5} torr to make metal–material–SnO_2 sandwich type cells. The thickness and area of the films were 20 to 25 μm and 2 cm^2 respectively. These sandwiched cells were put in a conductivity cell. The current measurement were taken with a Keithley 610 C electrometer.

The absorption spectra were recorded on a Perkin–Elmer 590B spectrophotometer. The cells were illuminated by a halogen lamp and the intensity was varied by changing the bulb to sample spacing and monitored by a solar meter. The capacitance measurements were done on the *C–V* plotter with fixed frequency.

3. Results

3.1. Electrical and photoconductivity studies

The variation of log *J* against log *E* in the dark for EBBB and AgBr–EBBB is shown graphically in Fig. 1. It can be seen that the current density in all cases increases with the electric field for all temperatures in the range of 40 to 120 °C.

There is linear dependence of current density with electric field. However, the gradient keeps on increasing, as we increase the temperature. At low temperatures the graident is 1.0 indicating Ohmic behaviour. When the temperature is increased the gradient of the log *J* against log *E* curve increases to 1.7 at 120 °C. The effective potential barrier height (ϕ') between

0022–2461/91 $03.00 + .12

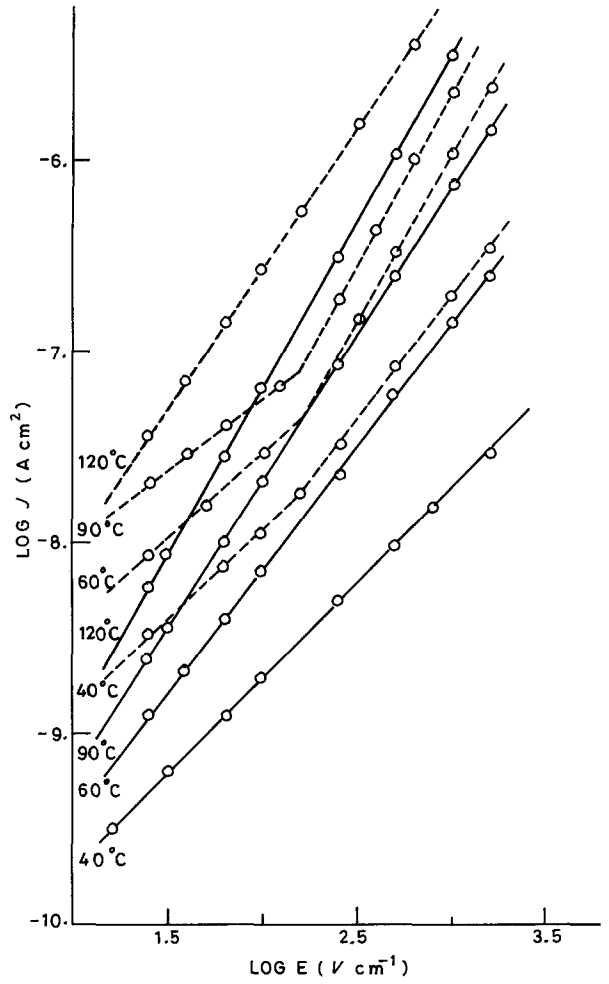

Figure 1 Variation of current density J with electric field E in the dark at different temperatures. (—— EBBB, – – – AgBr-EBBB).

metal and dye has been obtained from the slope of plot of log J/T^2 against $1/T$ (not shown here) and collected in Tables I and III.

The value of the potential barrier height decreases of sensitization and also as the work function of the metal electrode is increased.

The results of dark and photoconductivity at room temperature for pure and sensitized dyes for different electrodes are collected in Table II. The variation of dark and photoconductivity with $1000/T$ for pure and CdS sensitized RB (for example) are shown in Fig. 2. The log σ against $1000/T$ curves are composed of two straight lines. The activation energies of conduction obtained from the slopes of the above plots are collected in Tables I and III.

3.2. Photovoltaic effect

The absorption and action spectra of pure and sensitized EBBB and RB dyes are shown in Fig. 3. It can be seen from these figures that the absorption peak shifted toward the shorter wavelength region after sensitization. In the case of CdS sensitized RB we obtain a broad absorption band encompassing 400 to 600 nm with one maximum around 510 nm. This clearly indicates a strong molecular interaction between CdS and RB molecules. The I–V characteristics of SnO_2–EBBB–CdS–Ag and SnO_2–EBBB–AgI–Ag sandwiched cells are shown in Fig. 4 in both in the dark and illuminated. It is clear from these figures that these sandwiched cells show rectifying properties indicating a forward biased junction. On illumination

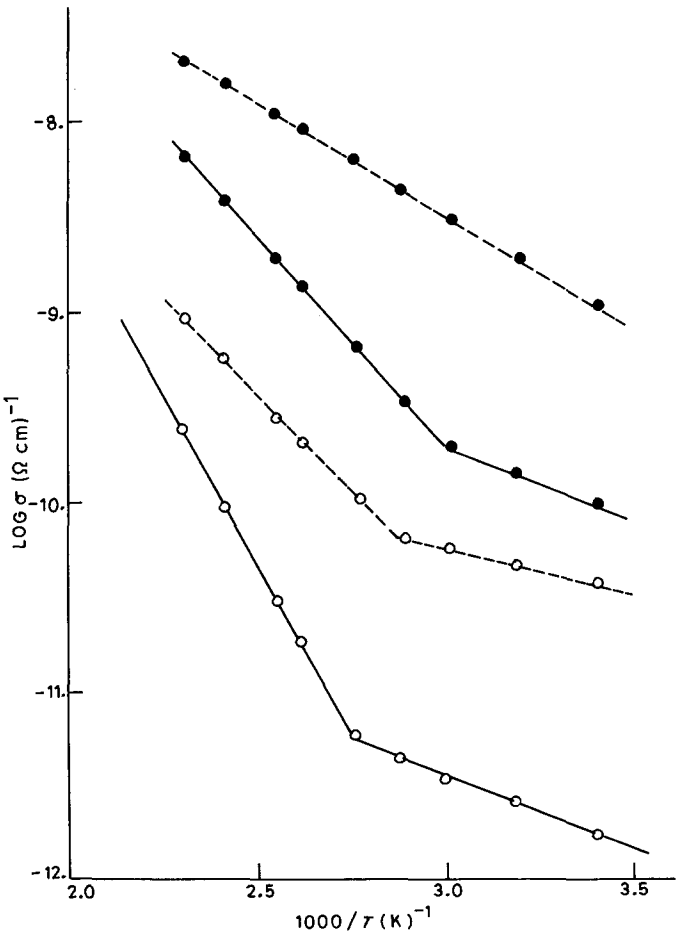

Figure 2 Variation of log σ with $1000/T$ in dark (——) and light (– – –) (○ RB, ● CdS-RB).

TABLE I Potential barrier height (ϕ') and activation energy in dark using different electrodes

Dyes and sensitized dyes	Potential barrier height in dark in (eV)			Activation energy in dark in (eV)		
	Al	Ag	Cu	Al	Ag	Cu
Pure EBBB				1.33	1.20	1.09
CdS–EBBB	0.93	0.87	0.81	0.72	0.68	0.58
AgBr–EBBB	1.37	1.34	1.27	1.13	1.02	0.95
Pure RB	–	0.60	0.54	–	1.02	0.95
CdS–RB	–	0.52	0.48	–	0.78	0.71

TABLE II Dark and photoconductivity at room temperature using different electrodes

Dye and sensitized dye	Dark conductivity ($\Omega^{-1}\,cm^{-1}$)			Photoconductivity ($\Omega^{-1}\,cm^{-1}$)		
	Al	Ag	Cu	Al	Ag	Cu
Pure EBBB	3.81×10^{-13}	8.9×10^{-13}	5.1×10^{-11}	1.17×10^{-11}	7.15×10^{-11}	1.6×10^{-10}
CdS–EBBB	3.4×10^{-9}	7.8×10^{-9}	1.5×10^{-8}	8.4×10^{-8}	1.34×10^{-7}	5.1×10^{-7}
AgBr–EBBB	5.1×10^{-10}	9.7×10^{-10}	8.1×10^{-9}	5.6×10^{-9}	9.11×10^{-9}	8.1×10^{-8}
Pure–RB		1.02×10^{-12}	5.20×10^{-11}		8.9×10^{-11}	1.55×10^{-10}
CdS–RB						

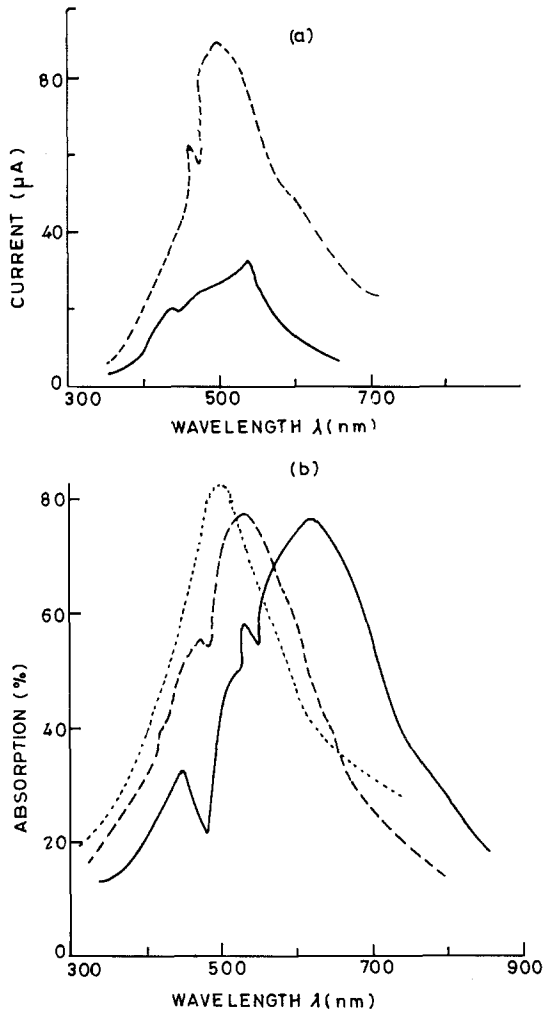

Figure 3 Absorption and spectral response curves for different cells (a) —— AgI-EBBB, --- CdS-EBBB. (b) — EBBB, ---AgI-EBBB, ----CdS-EBBB.

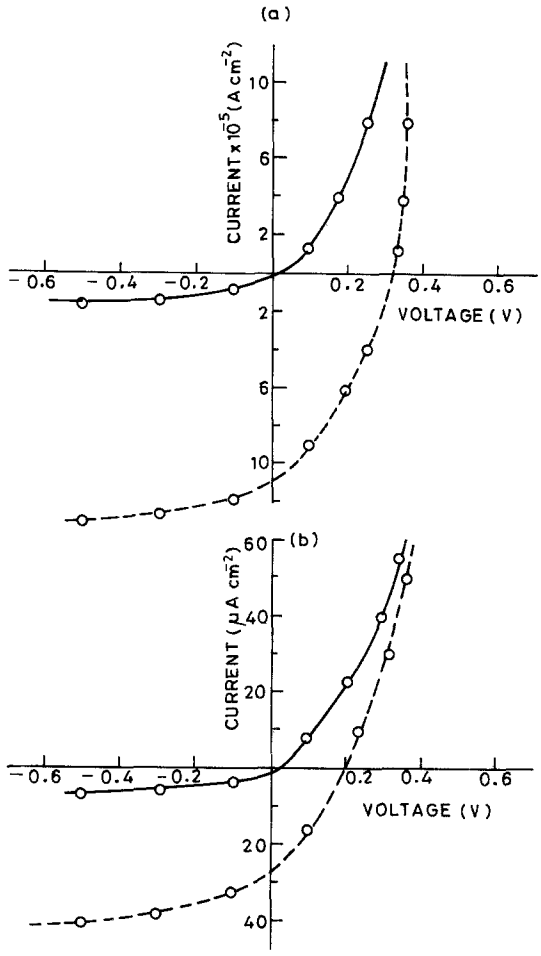

Figure 4 Photovoltaic I–V characteristics, (a) SnO_2–EBBB-CdS-Ag, (b) SnO_2–EBBB-AgI-Ag.

the SnO_2 electrode develops a positive polarity of generated photovoltage which indicates that the forward current is due to the hole injection from SnO_2 [15].

The variation of photocurrent with photovoltage by varying load resistors at constant intensity for the above sandwiched cells is shown in Fig. 5.

The variation of short circuit current (J_{sc}) and open circuit voltage (V_{oc}) with intensity for these sandwiched cells is shown in Fig. 6. In the case of EBBB and

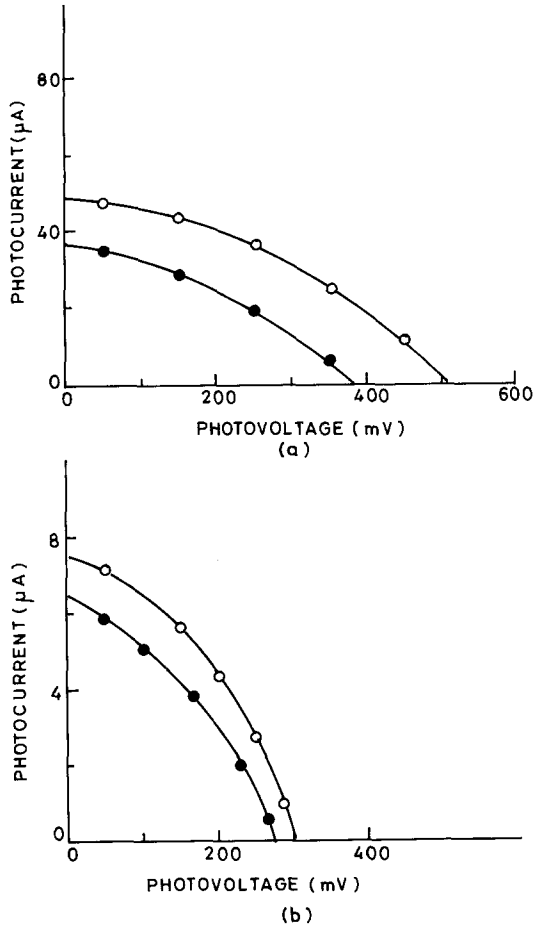

Figure 5 Variation of photocurrent with photovoltage for different sandwiched cells. (a) ○ Cu–CdS-RB–SnO_2, ● Ag–CdS-RB–SnO_2, (b) ○ Cu–RB–SnO_2. ● Ag–RB–SnO_2.

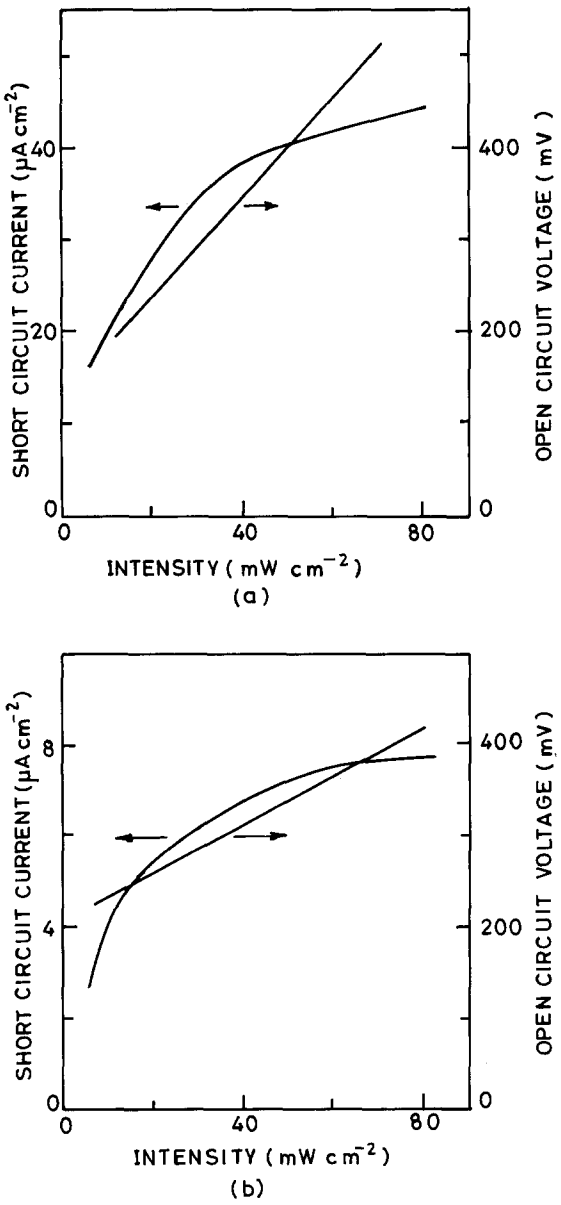

Figure 6 Variation of J_{sc} and V_{oc} with intensity. (a) Ag–CdS-RB–SnO_2, (b) Ag–RB–SnO_2.

CdS–EBBB, short circuit current varies as $I_{sc} \propto F^t$ (where F is the incident light intensity and t a factor which varies between 0.5 and 1.0) at high intensity. This variation of photocurrent is affected by an exponential trap distribution [16]. In the case of RB and CdS–RB the short circuit current varies as $I_{sc} \propto F^{1/3}$. This dependence of I_{sc} on intensity is because when the light is sufficiently high, the photogenerated carriers in the surface region are larger than those present at thermal equilibrium [16].

The Schottky barrier capacitance in metal–pure dye–SnO_2 and metal–sensitized dye–SnO_2 sandwiched cells as a function of the bias voltage was measured at various fixed frequencies in the dark and is shown in Fig. 7. The slope of the $1/C^2$ against V plot is related to the space charge density N in the depletion region and is given by [12]

$$\frac{d}{dV}\left(\frac{1}{C^2}\right) = -\frac{2}{\varepsilon\varepsilon_0 eN}$$

The intercept of the $1/C^2$ against V plots on the voltage axis measure the junction potential or built-in potential. These plots show a linear relationship which implies uniform doping in the junction region for the Schottky barrier device except CdS–Rb.

TABLE III Activation energy and potential barrier height in light using different electrodes

Dye and sensitized dye	Potential barrier height (eV)			Activation energy in (eV)		
	Al	Ag	Cu	Al	Ag	Cu
Pure EBBB				–	0.89	0.81
CdS–EBBB		0.68	0.63	–	0.49	0.45
AgBr–EBBB		0.89	0.84	–	0.75	0.70
Pure–RB	0.30	0.26	–	0.70	0.64	0.60
CdS–RB	0.26	0.21	–	0.46	0.40	0.36

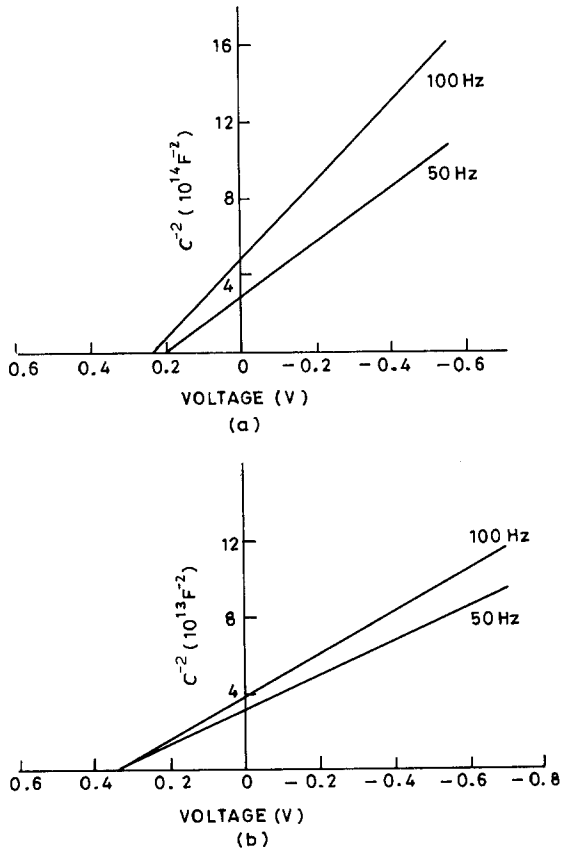

Figure 7 C–V characteristics for different cells in dark. (a) Ag–EBBB-AgI–SnO_2, (b) Ag–EBBB–CdS–SbO_2.

4. Discussion

4.1. Electrical properties

The change in the slope of the log J and against log E curve may be attributed to the injection of charge carriers into the dye. Since we do not observe any field dependent conduction process, we can say that the carriers are supplied by the impurity present in the dye. In AgBr sensitized EBBB, at low temperature there is a transition from Ohmic to space charge limited current region, while at high temperature this transition disappeared. This disappearance of transition at high temperature may be attributed to the injection of charge carriers from impurities at high temperatures even at low fields.

The values of activation energy (ε) are collected in Tables I and III. The high value of activation energy in the high temperature region suggests conduction is intrinsic, the lower value of activation energy in the low temperature region may be due to the presence of some impurity states in between the conduction and the valence band.

The increase in conductivity on illumination is due to the generation of Frankel excitons, which are dissociated near the interface between metal and dye. This fact is also supported by our observation that the action spectra matches closely with the absorption spectra [14] (Fig. 3).

It is observed that both potential barrier height and activation energy decrease on sensitization. Shifting of Fermi level toward conduction band on sensitization is a possible reason for this [14]. The increase in conductivity on sensitization may be due to the fact that the inorganic sensitizer ion acts as an electron donor and injects free charge carriers into the dye, thereby increasing the total carrier concentrations in the system.

4.2. Photovoltaic effect

The photovoltaic parameters like short circuit current (J_{sc}) open circuit voltage (V_{oc}), fill factor (FF) and power conversion efficiency (η) were calculated by analysing the photocurrent–photovoltage data and are collected in Table IV. The fill factor and conversion efficiency are given by

$$FF = (J_{max}V_{max})/(V_{oc}J_{sc})$$

$$\eta(\%) = \frac{J_{sc}V_{oc}FF \times 100}{F}$$

where J_{max} and V_{max} are photocurrent and photovoltage at maximum power output respectively and F is incident light intensity.

It is found that both J_{sc} and V_{oc} increase on sensitization and on using a high work function metal electrode. This effect is due to the fact that a high work function metal forms a contact of lower potential barrier height with dye than that for lower work function metal. Hence a large number of charge carriers cross the barrier to take part in the conduction.

TABLE IV Photovoltaic parameters for different sandwich cells

Cells	V_{oc} (mv)	J_{sc} ($A \times 10^{-6}$)	FF	η (%)	J_0 ($A\,cm^{-1}$)	n	ϕ (%)
Ag/AgI-EBBB/SnO_2	200	2.90	0.43	0.034	1.1×10^{-9}	2.6	0.18
Ag/CdS-EBBB/SnO_2	315	115	0.43	0.040	1.2×10^{-8}	2.4	0.76
Ag/RB/SnO_2	275	6.30	0.43	0.0022	1.8×10^{-9}	4.2	3.0×10^{-2}
Ag/RB-CdS/SnO_2	375	37.0	6.44	0.017	2.3×10^{-8}	3.1	0.020
Cu/RB-CdS/SnO_2	510	49.0	0.45	0.032	5.3×10^{-8}	3.9	0.029

V_{oc} Open circuit voltage
J_{sc} Short circuit current
FF Fill factor
η(%) Conversion efficiency
J_0 Reverse saturation current
n Diode factor
ϕ Quantum collection efficiency.

The quantum collection efficiency $\phi(\%)$ can be calculated according to

$$\phi(\%) = \frac{J_{sc} \times 1.24}{F \times (\mu m)}$$

The values of ϕ have been collected in Table IV. It is found that the ϕ depends on the back biasing voltage at low intensities. This behaviour suggests that the photocurrent in the cell is generated through the dissociation of excitons at metal–dye interface formed by light excitation.

The $1/C^2$ against V plots indicate that the space charge density in the depletion region also varies with the frequency. The difference in space charge density on sensitization is due to the variation of trap density at the surface during the sensitization process.

As we know, the space charge width, W, at the metal–semiconductor interface can be deduced from the relation $W = (2\varepsilon\varepsilon_0/qN)^{1/2}$. On sensitization the depletion layer width (W) decreases, leading to a strong electric field near the interface which rapidly separates the excitons into free electron and holes. This increases the conductivity and overall efficiency.

5. Conclusion

It may be concluded that the sensitization process plays a dominant role in the conduction mechanism and photovoltaic behaviour of organic dyes. The present quantum collection efficiency and fill factor can be improved by proper sensitization. The series resistance of these cells is still the limiting factor. The construction of thinner cells and proper sensitization of organic dye to increase the conductivity and fill factor are two approaches currently being studied to improve the power conversion efficiency.

References

1. R. B. CHAMP and M. D. SHATTUCK, US Patent 3 824 099 (1974).
2. H. W. ANDERSON and M. T. MOR, US Patent 4 140 987 (1979).
3. G. D. SHARMA, A. K. TRIPARTHI, D. C. DUBE and S. C. MATHUR, *J. Phys. Appl. Phys.* **16** (1983) 1977.
4. V. B. JIPSON and C. R. JONES, *J. Vac. Sci. Technol.* **18** (1981) 105.
5. V. Y. MERRITT and H. J. HOVEL, *Appl. Phys. Lett.* **29** (1976) 414.
6. R. O. LOUTFY, *Can. J. Chem.* **59** (1981) 549.
7. S. KANAYEMA, M. HIROI, N. OKUYEME and H. YASUNEGE, *Jpn J. Appl. Phys.* **22** (1983) 348.
8. R. O. LOUTFY and C. K. HSIAO, *Can. J. Phys.* **59** (1981) 727.
9. F. R. FAN and L. R. FAULKNER, *J. Chem. Soc.* **101** (1979) 4779.
10. G. A. CHEMBERLEIN and R. E. MALPAS, *J. Chem. Soc. Faraday Discuss.* **70** (1981) 299.
11. R. O. LOUTFY, Y. H. SHING and D. K. MURTI, *Solar Cells* **5** (1982) 331.
12. G. A. CHEMBERLEIN, *J. Appl. Phys.* **53** (1982) 6262.
13. T. SKOTHEIM, J. M. YANG, J. OTVOS and M. P. KELIN, *J. Chem. Phys.* **77** (1982) 6144.
14. H. MEIER, *J. Phys. Chem.* **69** (1965) 779.
15. G. D. SHARMA, D. C. DURE and S. C. MATHUR, *Solar Cells* **15** (1985) 189.
16. R. O. LOUTFY and J. N. SHARP, *J. Chem. Phys.* **71** (1979) 1211.

Received 8 February
and accepted 11 October 1988